UNIVERSITY OF ŽILINA

TRANSCOM PROCEEDINGS 2015

11-th EUROPEAN CONFERENCE OF YOUNG RESEARCHERS AND SCIENTISTS

under the auspices of

Tatiana Čorejová
Rector of the University of Žilina

SECTION 5

MATERIAL ENGINEERING MECHANICAL ENGINEERING TECHNOLOGIES

ŽILINA June 22 - 24, 2015
SLOVAK REPUBLIC

TRANSCOM 2015, 22-24 June 2015
University of Žilina, Žilina, Slovak Republic

Theoretical Model of the Laser Welding Process

[*]Rafał Banak, [*]Włodzimierz Zowczak, [**]Tomasz Mościcki
[*]Kielce University of Technology, Faculty of Mechatronics and Mechanical Engineering, Laser Processing Research Centre, al. Tysiąclecia Państwa Polskiego 7, 25-314 Kielce, Poland, {rbanak, wzowczak}@tu.kielce.pl
[**] Institute of Fundamental Technological Research Polish Academy of Sciences, Pawińskiego 5B, 02-106 Warsaw, Poland, tmosc@ippt.pan.pl

Abstract. To determine the distribution of the temperature field and the shape of the melting zone during the laser welding process of 304 stainless steel a three-dimensional numerical model was built and numerical simulation was performed. In order to improve the accuracy of the calculations temperature dependent material properties, heat loos due to the vaporization and heat exchange with surrounding medium due to the convection and radiation was considered.

Keywords: Computational Fluid Dynamics, Laser welding simulation, Finite Volume Method

1. Introduction

Nowadays laser beam is one of the highest power density sources available to industry [1]. Lasers are used to cut as well as to weld metals. In industrial applications CO_2 and solid state laser systems are most dominating [2]. There are two main types of laser welding: conduction mode and keyhole welding. Keyhole or deep penetration welding is commonly used to join thick elements. Due to the high power density joined metals begin to evaporate which leads to the formation of the plasma. Keyhole welding process is relatively unstable – welds often contains pores and spatters. Conduction mode welding occurs when power density does not excess 10^{10} W/m^2. That process is more stable than keyhole mode but on the other hand depth of welding is usually limited to hundreds μm.

Laser welding have many advantages over arc or gas metal arc welding process. Narrow heat affected zone and low distortions combined with precise laser beam delivery gives possibility to weld heat sensitive components and electronic parts. Often there are requirements imposed on the weld dimensions and maximum temperature – like for dissimilar materials welding where mixing zone size should allow materials to mix but at the same time the process temperature cannot exceed the boiling point of the component. One can predict laser welding process parameters basing on previously conducted experiments but this approach often requires many attempts and money consuming investigations.

A convenient alternative to relatively expensive destructive tests seems to be analytical [4][3] and numerical models. Since analytical approach has many limitations arising from unsteady nature of welding process, complex geometries and changing material properties numerical simulations are now major topic in most papers describing welding. Currently there are some software suits which are designed to perform numerical analysis of welding process. They are usually designed for industry use and offers ready solutions for common welding processes. On the other hand multiphysics suits offer the ability to create own heat sources and taking into account additional effects associated with welding like evaporation or turbulent flow in weld pool. In this paper for computation of temperature distribution and weld pool geometry commercial CFD software Ansys Fluent was used.

2. Mathematical model

Mathematical model used in numerical simulation describing interaction of the laser beam with the work piece consists of Fourier-Kirchoff and Navier-Stoke differential equations. For incompressible flow system of equation consists of [5]:

$$\frac{\partial \rho}{\partial t} + \nabla \cdot (\rho \vec{v}) = 0 \tag{1}$$

$$\frac{\partial \rho}{\partial t}(\rho \vec{v}) + \nabla \cdot (\rho \vec{v} \vec{v}) = -\nabla \rho + \nabla \cdot \left(\overline{\overline{\tau}} \right) + \rho \vec{g} + \vec{F} \tag{2}$$

where p is the static pressure, ρ, g and F are the gravitational body force and external body forces and stress tensor $\overline{\overline{\tau}}$ is given by [5]:

$$\overline{\overline{\tau}} = \mu \left[\left(\nabla \vec{v} + \vec{v}^{\,T} \right) - \frac{2}{3} \cdot \vec{v} I \right] \tag{3}$$

where μ is the molecular viscosity and I is the unit tensor. Second right hand side of equation is the effect of volume dilation.

The turbulence kinetic energy, k, and its rate of dissipation ε, are obtained from the following transport equations [6]:

$$\frac{\partial}{\partial t}(\rho k) + \frac{\partial}{\partial x_i}(\rho k u_i) = \frac{\partial}{\partial x_j}\left[\left(\mu + \frac{\mu_t}{\sigma_k} \right) \frac{\partial k}{\partial x_j} \right] + G_k + G_b - \rho \varepsilon - Y_M + S_k$$

$$\frac{\partial}{\partial t}(\rho \varepsilon) + \frac{\partial}{\partial x_i}(\rho \varepsilon u_i) = \frac{\partial}{\partial x_j}\left[\left(\mu + \frac{\mu_t}{\sigma_\varepsilon} \right) \frac{\partial \varepsilon}{\partial x_j} \right] + C_{1\varepsilon} \frac{\varepsilon}{k}(G_k + C_{3\varepsilon} G_B) \tag{4}$$

$$- C_{2\varepsilon} \rho \frac{\varepsilon^2}{k} + S_\varepsilon$$

where G_k is generation of turbulence kinetic energy due to the mean velocity gradients, G_b – generation of turbulence kinetic energy due to buoyancy, Y_M is contribution of the fluctuating dilatation in compressible turbulence to the overall dissipation rate, $C_{1\text{-}3\varepsilon}$ – are the constants, σ_k and σ_ε – turbulent Prandtl numbers for k and ε (1.0 and 1.3 respectively) [7]. Due to the incompressible nature of welding process some elements of (4) are equal zero.

Laser heat source was built and included into computations in the following form [8]:

$$-k_{eff} \frac{\partial T_s}{\partial \vec{n}} = I_L \cdot A - \alpha (T - T_\infty) - \sigma \varepsilon_p \left(T^4 - T_\infty^4 \right) - \rho u(t) L_v \tag{5}$$

where L_v is heat of vaporization, $\vec{n}$ is the unit vector, α is external heat transfer coefficient, ε_p is emissivity of the external wall surface and σ is Stefan-Boltzman constant. Velocity of the evaporation front u is determined from the Hertz-Knudsen equation [9]:

$$u(T_s) = \frac{(1-\beta)}{\rho} \left(\frac{m}{2\pi k T_s} \right)^2 p_b \exp\left[\frac{L}{k} \left(\frac{1}{T_b} - \frac{1}{T_s} \right) \right] \tag{6}$$

where L is the heat of evaporation, T_b is the boiling point at pressure p_b=10^5 Pa and T_s is the surface temperature.

Boundary conditions at the surfaces which are not affected by the laser beam were included as follow:

$$-k_{eff} \frac{\partial T_s}{\partial \vec{n}} = \alpha (T - T_\infty) + \sigma \varepsilon_p \left(T^4 - T_\infty^4 \right) \tag{7}$$

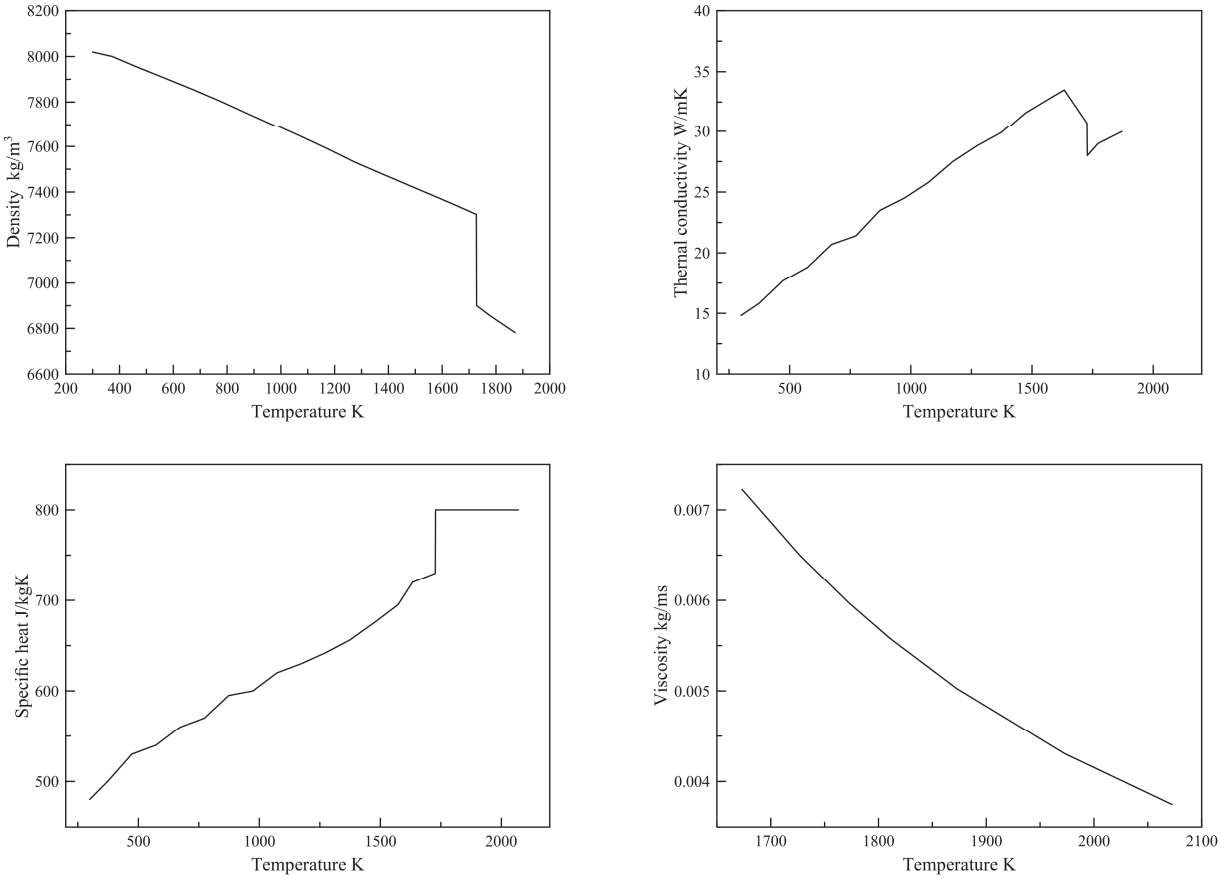

Fig. 1. Temperature dependent material parameters of 304 stainless steel [10].

As mentioned in melting and solidification process calculations it is important to take into account the temperature dependent material properties which are shown in Fig. 1. Assumed constant values are shown in Tab. 1.

Constant	Value
Melting heat	10^3 *J/kg*
Gas constant	8314.3 *J/kg mol K*
Liquidus temperature	1723 *K*
Solidus temperature	1658 *K*
Vaporization temperature	3135 *K*
Reference temperature	300 *K*
Reference pressure	$1.013*10^5$ *Pa*
Mole mass	55.8 *g/mol*
Stefan-Boltzman constant	$5.67*10^{-8}$ *W/m^{2}T^4*
Heat of vaporization	$6.09*10^6$ *J/kg*
Emissivity	0.4

Tab. 1. Constant values used in computations.

Due to the large temperature gradients denser mesh was created along laser path and close to the surface affected by laser beam. Rectangular computational domain, shown in Fig. 2, with 4x4x2 mm with 850000 cells was created. To compromise between the accuracy and duration of calculations, the time step between the iteration was set to $2.5 \cdot 10^{-5}$ s.

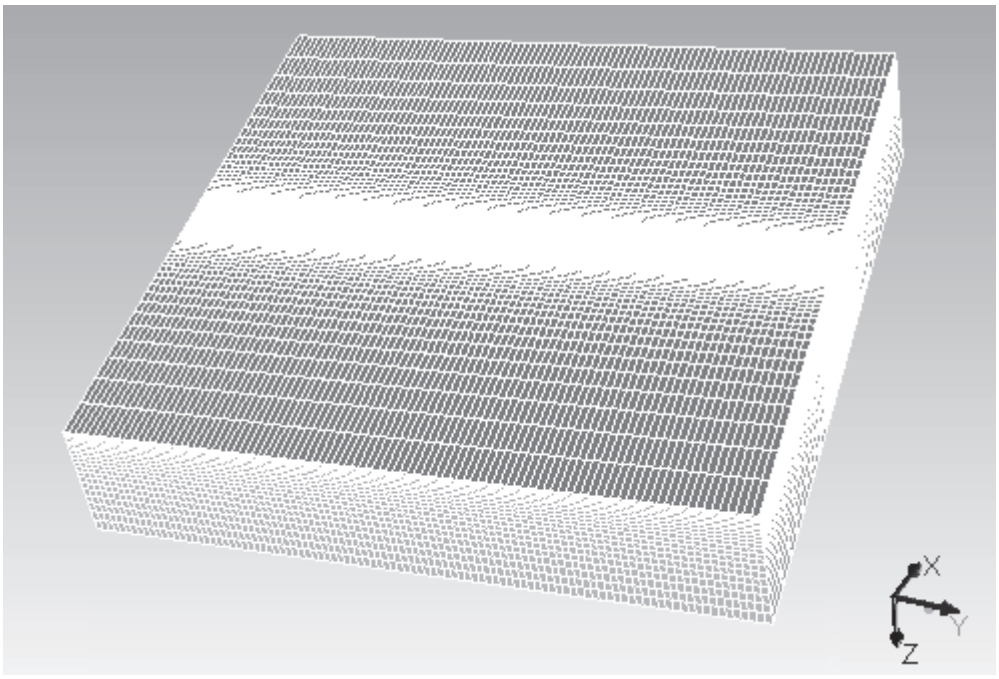

Fig. 2. Computational domain created for finite volume method calculations.

3. Numerical simulation results

For the calculations laser power P = 4000 W, laser spot diameter d = 0.5 mm, absorption coefficient κ = 0.05 and welding speed V = 2 m/min in Y direction were assumed. Surface tension phenomenon has a major influence on weld pool geometry – especially in the case of conduction mode welding. Presented model takes into account the Marangoni stress phenomenon with surface tension coefficient equal to 0.00049 N/m·K [11]. Negative surface tension coefficient values turns the motion of liquid steel in the weld poll inward to outward.

Fig. 3 shows molten pool geometry and temperature distribution in cross-section parallel to welding direction at time = 0.062 s and at center point X = 0.002 m Y = 0.002 m. Plots are focused on laser beam affected area. Fractional values on liquid fraction plot indicates existence of so called mushy zone. It's the area where iron is partially melted.

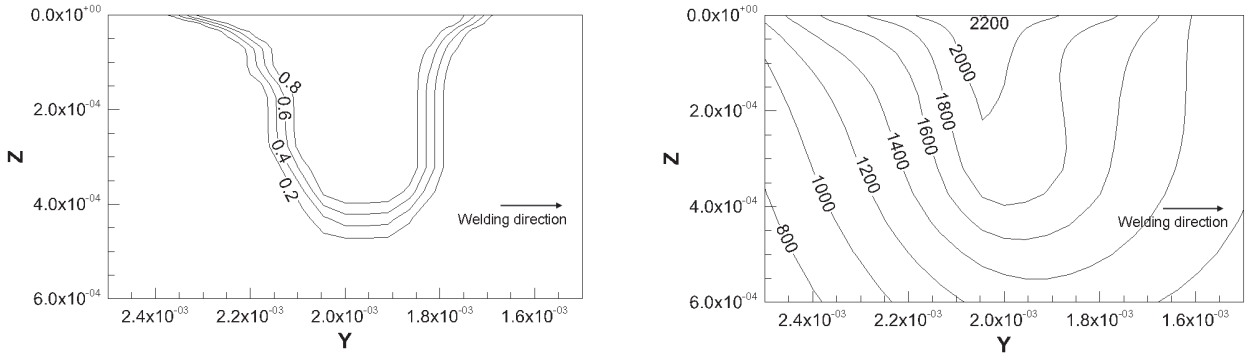

Fig. 3. Liquid fraction of molten iron (left) and temperature distribution (right) in cross-section parallel to welding direction.

Fig. 4 shows molten pool geometry and temperature distribution in cross-section plane perpendicular to the welding direction in same point as in Fig. 3. Maximum penetration depth for given parameters is equal to 420 μm while face of the weld has 525 μm width.

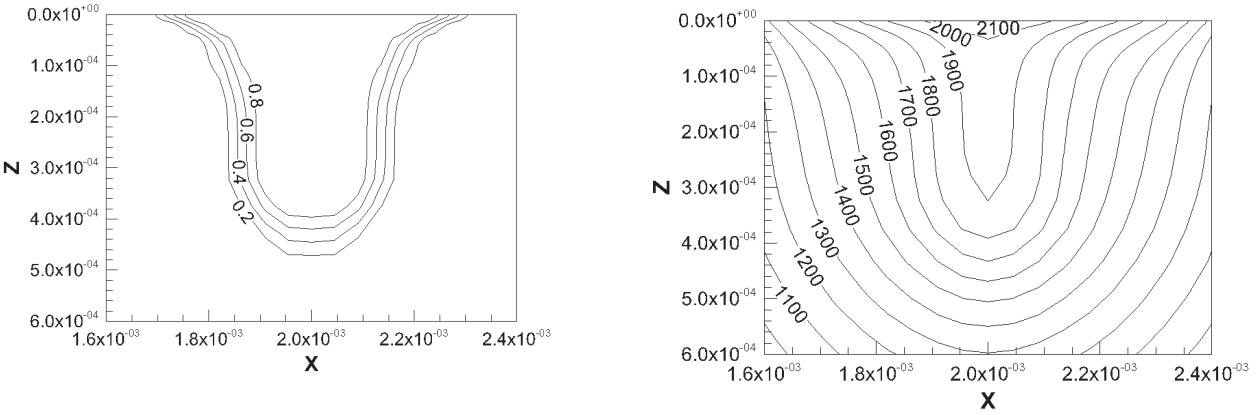

Fig. 4. Liquid fraction of molten iron (left) and temperature distribution (right) in cross-section perpendicular to welding direction.

Fig. 5 shows temperature distribution along laser beam path. Maximum temperature obtained from calculation was ~2200 K which is much lower value than vaporization temperature of stainless steel 304. This is important due to the fact that the exceeding of the boiling and evaporation temperature of the material usually results in a transition in to keyhole welding.

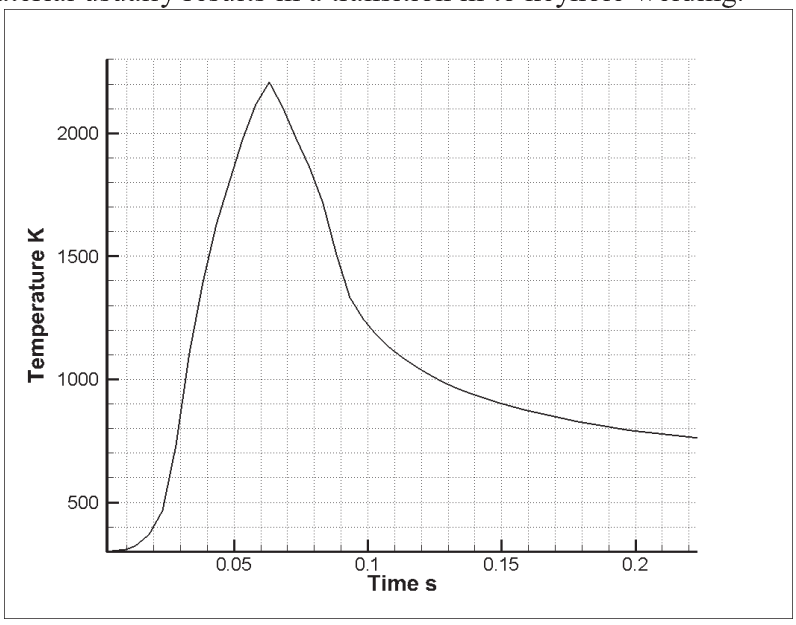

Fig. 5. Temperature distribution with respect to time at point X = 0.002 m Y = 0.002 m.

4. Conclusion

Due to the complexity of laser welding process the Ansys Fluent software has been utilized. The objective of the study was to build numerical model by means of which temperature distribution and welding pool geometry can be determined. In non-linear, transient heat and mass transfer analysis a three-dimensional model with a moving heat source was considered. Phase change phenomenon has been connected with a non-linear temperature-dependent material properties, metal evaporation heat loos model and heat exchange with surrounding medium in order to get results as close to the real as possible. User defined functions has been written to ensure more comprehensive control over laser spot size and power density.

Although described case need experimental verification it's in good agreement with similar already carried out joints. It seems that the numerical simulation is a convenient tool for prediction of laser beam welding. It can be successful employed in cases where the combined materials are expensive to reduce costs of determination of optimal process parameters. Proposed model can be easily adapted to different materials or heat sources (different lasers or welding methods).

Acknowledgement

This research was supported in part by PL-Grid Infrastructure. This work was supported by National Centre for Research and Development (NCBiR) contract number PBS1/B5/13/2012

References

[1] W. M. Steen and J. Mazumder, *Laser Material Processing*. 2010.

[2] M. Turňa, B. Taraba, P. Ambrož, and M. Sahul, "Contribution to Numerical Simulation of Laser Welding," *Phys. Procedia*, vol. 12, pp. 638–645, 2011.

[3] W. Zowczak, "Uproszczone pole temperatury dla analizy procesu spawania laserowego," *Przegląd Elektrotechniczny*, vol. 07, p. 76, 2011.

[4] B. Grabas and E. Mazur, "Obliczenia teoretyczne kształtu laserowej spoiny punktowej," *Przegląd Elektrotechniczny*, vol. R. 84, nr , pp. 126–128, 2008.

[5] Ansys, "ANSYS FLUENT theory guide," 2009.

[6] N. Chakraborty, "The effects of turbulence on molten pool transport during melting and solidification processes in continuous conduction mode laser welding of copper–nickel dissimilar couple," *Appl. Therm. Eng.*, vol. 29, no. 17–18, pp. 3618–3631, Dec. 2009.

[7] B. E. Launder and D. B. Spalding, *Lectures in Mathematical Models of Turbulence*. London: Academic Press, 1972.

[8] T. Mościcki and J. Radziejewska, "Numerical simulation and experimental analysis of simultaneous melting and burnishing of 304 stainless steel with oscillatory laser heat source," *Kov. Mater.*, vol. 51, no. 1, pp. 37 – 44, 2013.

[9] A. V Bulgakov and N. M. Bulgakova, "Thermal model of pulsed laser ablation under the conditions of formation and heating of a radiation-absorbing plasma," *Quantum Electron.*, vol. 29, no. 5, pp. 433–437, May 1999.

[10] K. C. Mills, *Recommended values of thermophysical properties for selected commercial alloys*. Cambridge: Woodhead Publishing, 2002.

[11] T. Matsumoto, T. Misono, H. Fujii, and K. Nogi, "Surface tension of molten stainless steels under plasma conditions," *J. Mater. Sci.*, vol. 40, no. 9–10, pp. 2197–2200, May 2005.